CHAPTER 1

INTRODUCTION AND REVIEW OF LITERATURE

1.1 INTRODUCTION AND SCOPE

Rapid increase in transistor density and decrease in size of integrated circuits have led to the generation of high heat fluxes and associated hot spots (Peterson 1994; Faghri 1995; McGlen 2006). The resulting high temperature leads to the deterioration of the performance of electronic devices including mechanical failures due to uneven stress development (Dunn and Reay 1982; Peterson et al. 1990; Stephan and Busse 1992; Peterson 1992; Peterson et al. 1993; Peterson 1994; Faghri 1995; Ma and Peterson 1997; Andrews et al. 1997; Lee 2010). Thus, it is necessary to develop new thermal management strategies for electronic devices capable of removing heat at very high flux rates and increasing the mean-time-between-failure of these devices. Heat pipes have gained prominence in this regard, primarily owing to their compact sizes, on-board integrability and enhanced cooling performance (Peterson 1994; Groll et al. 1998; Gromoll 1998; Faghri 1995; Chen et al. 2009; Ohadi 2005).

Conventional heat pipe is a closed device where liquid and its vapor coexist and travel in opposite directions inside the heat pipe (Ranjan et al. 2009). The liquid travels towards the hot region through a wicking material provided along the periphery of the heat pipe. The vapor, generated by the phase change of the coolant liquid at the heated section, travels through the central core towards the cooler region. The heat pipe can be divided into three zones, namely the evaporator, adiabatic and condenser sections. The evaporator end of the heat pipe is kept in contact with the heat producing device. The liquid at the hot end is heated by the thermal energy dissipated from the device, and gets evaporated. The higher pressure at the evaporator section drives the vapor towards the cold end where it condenses, releasing the heat at the condenser end. The condensed liquid, due to the capillary action provided by the wick material along the periphery, travels back to the hot end to replenish the amount evaporated (Ranjan et al. 2011, 2012). The adiabatic zone is characterized by negligible transport across the phases and the temperature remains nearly constant.

The evaporation, condensation and transport within the heat pipe run in a cyclic process. Hence, no extra liquid is needed from the outside, once the heat pipe is charged with the appropriate amount of coolant liquid and is sealed (Dunn and Reay 1982; Peterson 1994; Faghri 1995). The schematic of a conventional heat pipe is shown in Figure 1.1.

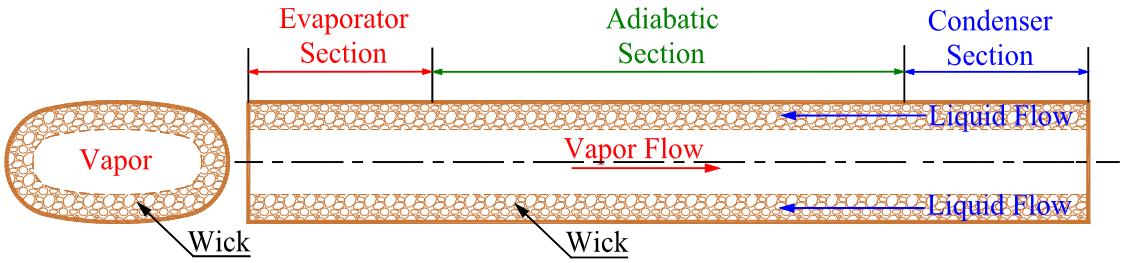

Figure 1.1. Schematic representation of working principle of a conventional (wicked) heat pipe

Since change of phase is exploited during the operation of a heat pipe, the amount of heat extracted from the hot regions can be significantly higher than the other conventional methods (which mostly use convection and conduction) and hence is ideally suited for thermal management (Peterson and Wu 1990; Wu and Peterson 1991; Wu et al. 1991; Kaviany 2001) with enhanced thermal conductivity and efficient heat spreading (Stephan and Busse 1992; Vafai and Wang 1992).

Conventional (wicked) heat pipes can easily be installed where packaging size is not of critical importance (Peterson et al. 1993). Further, the shape and size can be changed to fit the location and space available, and multiple evaporators can be connected with a single condenser using wings to cool an array of heat generating components at a time. There is no moving part except cooling fans supporting condenser, additional power is not required to run the heat pipe and this is simple, reliable, silent and maintenance free (Launay et al. 2004). The conventional heat pipe is widely used in large packaging systems, gravity based systems, solar industry and in many industrial cooling purposes (Silverstein 1992; Peterson 1994; Faghri 1995; Kim et al. 2003; Kirby 2010).

The presence of wicks in traditional heat pipes causes low form factor and large volume to surface area ratio that lead to inefficient control over the interfacial transport (Peterson et al. 1993; Suman et al. 2005). Further, due to the presence of the

porous structure along the entire length of the conventional heat pipe, as well as the viscous interaction between the vapor and the liquid phases, major pressure losses may develop with liquid flowing through it. The thermal performance of a heat pipe deteriorates as these losses adversely affect the heat transfer over a long distance (Wu and Peterson 1991; Suman et al. 2005a). Furthermore, the performance of a conventional heat pipe is appreciably affected by gravity. The overall pressure losses in these heat pipes result in lower efficiency of the heat transfer process. Additionally, the miniaturization of the semiconductor devices and the advent of high performance mobile computing platforms demand chip-cooling devices to have much smaller footprints, ranging from microns to millimeters with provision for on-chip integration. The limitations of the conventional heat pipes, in conjunction with the needs for miniaturization and improved thermal performance along with addressing the ever increasing heat-generation to heat-scavenging crossover barriers, have made micro heat pipes extremely relevant in the present scenario (Peterson et al. 1993; Hung and Tio 2012).

The concept of micro heat pipe was first proposed by Cotter in 1984 (Cotter 1984). He defined micro heat pipe as a device inside which the mean curvature of the vapor-liquid interface is necessarily comparable in magnitude to the reciprocal of the hydraulic radius of the total flow channel. The shape of the cross section should be convex but cusped (e.g. polygon), having a diameter in the range of 10 to 500 μm. Micro heat pipe essentially is a wickless heat pipe used to achieve uniform temperature distribution in micromechanical and microelectronic devices and in various other applications, where a high degree of temperature consistency and uniformity are required (Faghri 1995; Vafai and Wang 1992; Vafal et al. 1995; Zhu and Vafai 1998; Wang and Vafai 2000a, 2000b; Vasiliev 2008). Vapor and liquid flow inside rectangular and triangular micro heat pipes are schematically shown in Figure 1.2 and 1.3 respectively (Mghari et al. 2013; Peterson 1994). The long capillary of the micro heat pipe is filled with a liquid and a long vapor bubble. The bubble length is so big that it is comparable to that of the capillary. Cross sectional views reveal that the corners are covered by liquid menisci and vapor flows through the center. These corners act like capillaries and draw liquid from cold to hot end, primarily owing to the variation in liquid film curvature along the length of the heat pipe, functioning analogous to the porous structure of a conventional heat pipe. Liquid

near the hotspot gets vaporized and creates a high pressure zone that results in flow of vapor towards the colder end, which eventually releases latent heat as it condenses. Due to the high capillary forces, the corner channels keep supplying the condensed liquid back to the hot end to complete the cycle.

The micro heat pipes are especially suited for thermal control of microelectronic devices (Peterson 1992; Launay et al. 2004; Sashidhar et al. 2008). They are already in use for aircraft and spacecraft temperature control, thermal control of photovoltaic cells, laser diodes, solar cells, fuel cell applications and in applications related to bio and medical sciences (Peterson 1992; Faghri 1995; Vafai and Wang 1992; Zhu and Vafai 1998; Vafal et al. 1995; Wang and Vafai 2000).

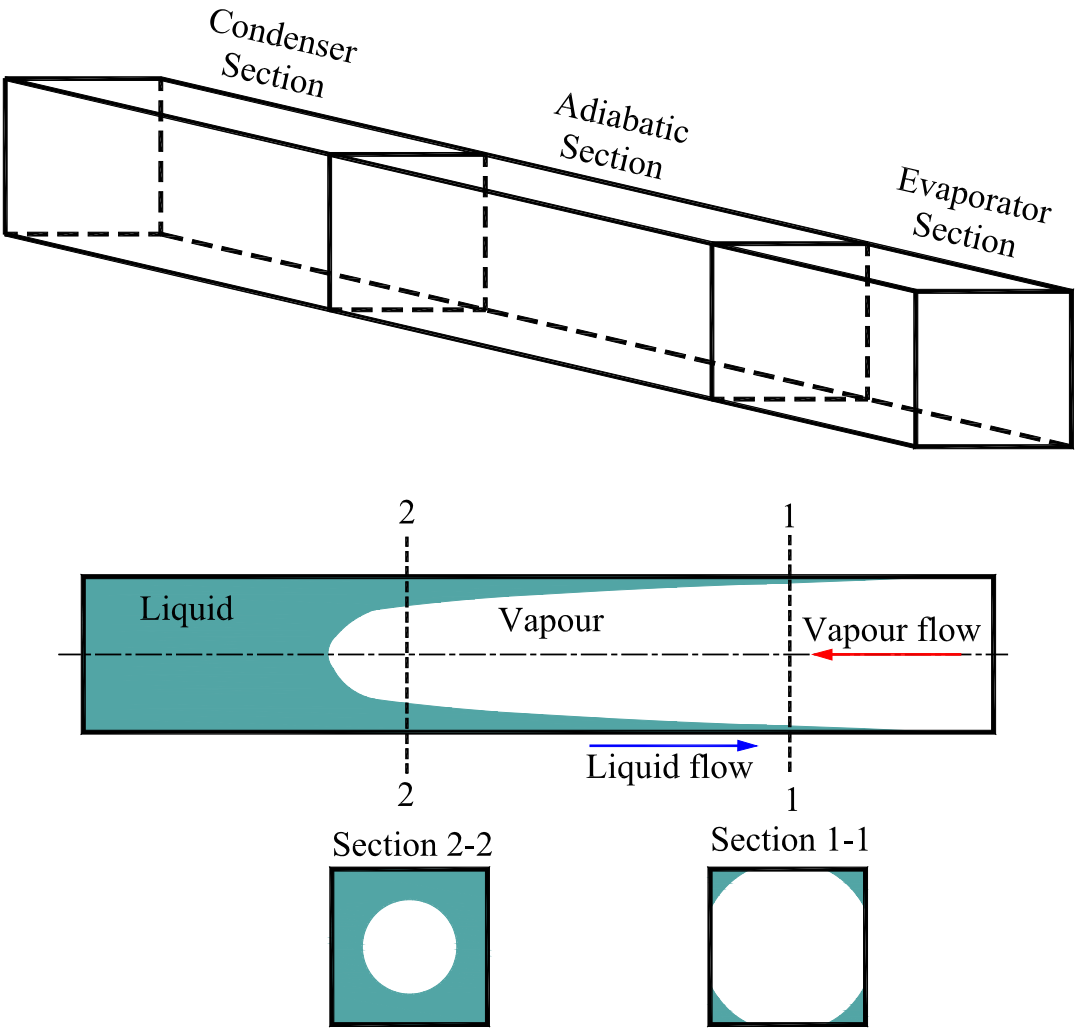

Figure 1.2. Schematic representation of working principle of a rectangular micro heat pipe

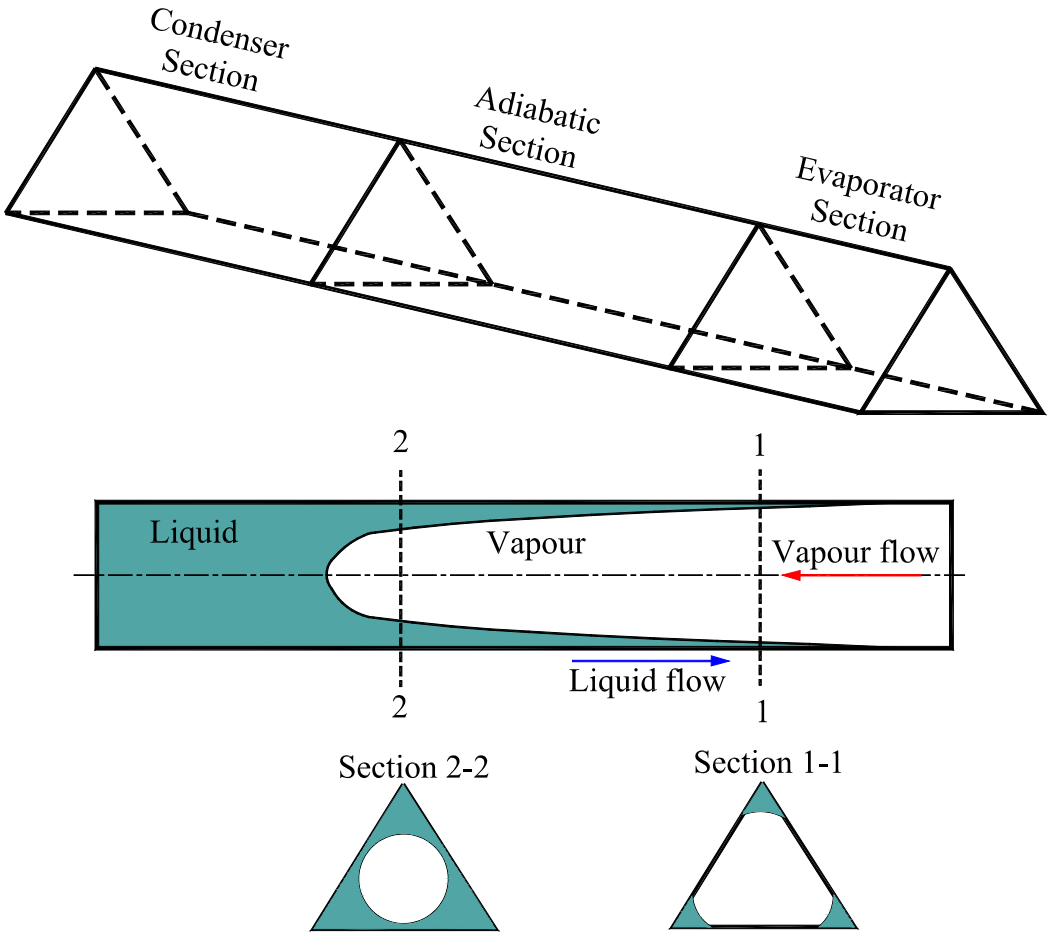

Figure 1.3. Schematic representation of working principle of a triangular micro heat pipe

1.2 PHYSICAL ISSUES

The fundamental physics governing the operation of micro heat pipe results from the difference in the capillary pressure across the liquid–vapor interfaces in the condenser and evaporator zone. Further, the performance greatly depends on the intermolecular interactions and wettability, as these microdevices exploit enhanced evaporation from the curved microfilms on the microchannel surfaces. Because of the presence of long range intermolecular forces and due to its curvature, the liquid thin film on a solid substrate has different free energy from that of a bulk fluid (Derjaguin and Churaev 1978; Deryagin et al. 1987; Peter and Wayner 1991; Park and Lee 2003; Park et al. 2003; Chakraborty and Som 2005; Panchamgam et al. 2005; Dhavaleswarapu et al. 2007; Kundu et al. 2011; Biswal et al. 2013; Pati et al. 2013). The key objective of this section is to present the concepts of intermolecular forces that play major roles in the thin film evaporation and provide suction towards the

contact line region of an evaporating thin film. A number of relevant interfacial phenomena, namely wettability, contact angles, capillarity, disjoining pressure, surface tension, contact line wetting principle, etc. will be discussed and their influences on the microscale heat transfer also will be probed. Wetting also plays an important role in many other industrial processes, such as lubrication, printing, liquid coating, spray quenching, oil recovery, etc.

The interaction between the coolant liquid and the solid depends strongly on the prevalent intermolecular forces. Intermolecular forces are defined as the attraction or repulsion between the neighboring atoms, molecules or ions. Intermolecular forces are weaker in comparison to the intramolecular forces of attraction as they typically involve smaller charges that are farther apart; however many of the bulk properties of matters in different phases are governed by intermolecular forces and hence these forces are important in the present study. Intermolecular forces may be classified into the following categories (Israelachvili 2011; Silberberg 2012).

Ion-dipole: Ion-dipole forces play a major role for the ionic compounds, which dissolve in water as these forces are the results of attraction between an ion and a nearby polar molecule.

Dipole-dipole: Dipole-dipole forces can be found in polar molecules. As the charges on the polar molecules are quite small, the dipole-dipole attractions are weaker in comparison to the ion-ion attractions.

Hydrogen-bond: Hydrogen bond is a special type of dipole-dipole force that occurs in a particularly special group of polar compounds, which are characterized by the X-H bond, where X can be O, N, or F.

Polarizability and Charged-Induced Dipole Forces: A nearby electric field that may be generated out of the electrodes of a battery, the charge of an ion, or the partial charges of a polar molecule, can distort the negatively charged electron clouds. This distortion creates a temporary induced dipole moment for non-polar molecules whereas for a polar molecule, it enhances the dipole moment already present. Polarizability is defined as the ease with which the electron cloud of a particle can be distorted.

Dispersion Forces: So far, the discussions of intermolecular forces were based on the existence of polarizability found either on the ion or polar molecules where charges exist. However, for nonpolar substances like chlorine, gasoline, octane, toluene, argon, etc. there are also intermolecular forces that cause these substances to condense and solidify. The intermolecular force, which is primarily responsible for the condensed states of nonpolar substances, is the dispersion force or London dispersion force (or London force, named after the physicist Fritz London, who explained the quantum-mechanical basis of the attraction). Instantaneous oscillations of electron charge in all kinds of atoms develop dispersion forces and hence, these forces exist between all particles e.g. atoms, ions, molecules. This is the only force that exists in nonpolar substances and it also exists in addition to other intermolecular forces in polar substances. For a nonpolar substance, e.g. argon, the atoms are close together and the instantaneous dipole in one atom induces a dipole in its neighbor resulting in an attraction between the two atoms owing to synchronized motion of the electrons in the two atoms. These attraction forces between atoms span throughout the sample. These attractions are capable to keep all the atoms together at low enough temperature. Thus, the dispersion forces are also induced dipole-induced dipole forces.

The dispersion force is the most dominant one amongst all the intermolecular forces except where polar molecules are present with large dipole moments or those forming strong Hydrogen bonds (Israelachvili 2011; Silberberg 2012; Kryukov et al. 2013). In contrast to the other types of forces that may or may not act depending on the characteristics of the molecules, dispersion forces play a role in a host of important phenomena such as cohesion, adhesion, physical adsorption, surface tension, the properties of the gases and liquids, aggregation of particles in aqueous solutions, structure of proteins and polymers where molecules are in condensed state (DasGupta 1992).

Based on the operating ranges, the intermolecular forces can be categorized as long range and short range forces. Long ranges forces are considered to be operating in a distance typically ranging from 1 nm to 100 nm whereas short range forces are assumed to be operating in one or two atomic distances. Short range forces are, in general stronger and sometimes dominate over the long range intermolecular forces.

The examples of short range forces are hydrogen bonds, chemical bonds, metallic bonds etc. Long range forces include dispersion forces, Keesom dipole-dipole forces and Debye dipole-induced dipole forces, which are collectively known as van der Waals forces. The presence of long range intermolecular forces can change the free energy of an ultra-thin film of liquid on a solid substrate significantly from that of the bulk fluid as these are functions of the thickness and curvature of the liquid film (Derjaguin and Zorin 1957; Deryagin and Churaev 1976; Derjaguin et al. 1965; Ludviksson and Lightfoot 1971; Wayner et al. 1976; Schonberg et al. 1995; Panchamgam et al. 2005; Truong and Wayner 1987; DasGupta et al. 1993; Ha and Peterson 1996; Suman et al. 2005b; Mandel et al. 2011).

Heat transfer capacity using thin film of a given liquid greatly depends upon the contact angle (wettability) that is generated in presence of interfacial tension resulting from the intermolecular forces. Figure 1.4 shows the pictures of the droplets of a liquid on different homogeneous horizontal surfaces using an advanced goniometer. Contact angle (θ) is the angle formed by the interaction of solid-liquid interface (SL) and the liquid-vapor interface (LV) as shown in the Figure 1.4(a). Geometrically, the liquid-vapor interface line at the three phase contact line is characterized by drawing a tangent line from the contact point along the liquid-vapor interface in the droplet profile. Three phase contact line is defined as the interface where the vapor, liquid and solid phases co-exist. Small contact angle implies large spreading. For complete wetting of the liquid on a given surface, the droplet of the liquid spreads flat on the surface and hence, the contact angle becomes 0°. Conventionally, the wetting is assumed to be favorable if the fluid spreads over a large area on the surface and the resulting contact angle is less than 90°. Such a surface is called hydrophilic surface. The wetting is considered to be unfavorable when the contact angle is greater than 90° and the surface is designated as hydrophobic surface. Additionally, the contact angle is not only relevant when a single liquid interacts with solid and vapor, it is also important in case of liquid-liquid interfaces. The liquid-vapor or liquid-liquid interface is always under stretched condition implying the existence of tensile force on the surface. The magnitude of this force per unit length of an imaginary line drawn along the interface is known as the surface tension coefficient or simply surface tension. Surface tension plays a major role in determining the shape of the liquid-liquid interface and the resulting shape of the

liquid droplet. The phenomenon of surface tension is resulted from the presence of inter molecular forces namely cohesion and adhesion. Cohesion is the force of attraction between the molecules of a liquid by virtue of which they are bound to each other to remain as one assemblage of particle and this force enables the liquid to resist tensile stress. Adhesion, on the other hand, is the force of attraction between unlike molecules, i.e., between the molecules of different liquids or between the molecules of liquid and those of a solid body when they are in contact with each other. Gravity, magnetic field (for magnetic fluid), electric field, etc. may deform the shape of the droplet and consequently the contact angle is determined by the confluence of surface tension forces and the other externally applied forces. Contact angle for a given solid-liquid system is also expected to be the function of the environment (Snoeijer and Andreotti 2008).

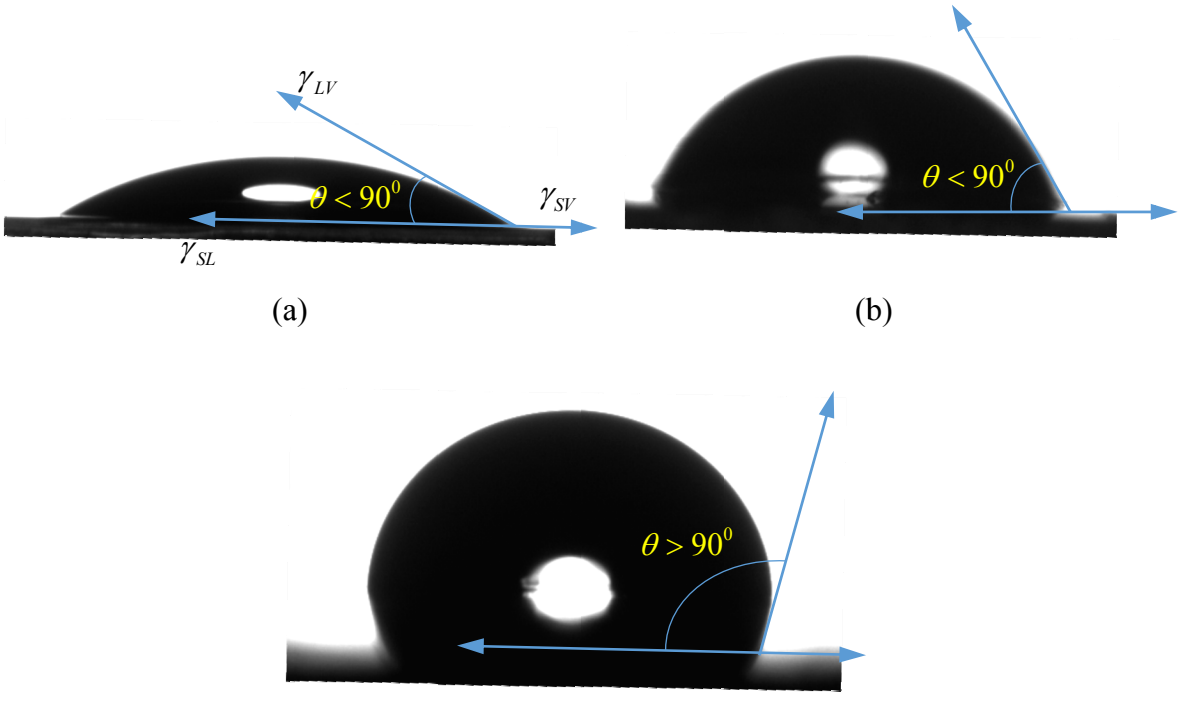

Figure 1.4. Contact angles of liquid on different homogeneous horizontal surfaces (a) Shape of a liquid droplet on a nearly wetting surface; (b) Shape of a liquid droplet on a partially wetting surface; (c) Shape of a liquid droplet on a hydrophobic surface

Young-Laplace equation $\left(P_v - P_l = \frac{\sigma}{R} \right)$ is used to delineate the pressure jump at the liquid-vapor interface, which is strongly influenced by the intermolecular and the surface forces present in the system. Here P_l and P_v are the liquid and vapor pressure respectively and R is the radius of curvature of the liquid. Wu and Peterson (1991) have shown that the pressure jump at the curved liquid-vapor interface during flow in microchannels is a function of the liquid-vapor surface tension and the interfacial radius of curvature. However, adhesion near the solid-liquid interface affects the stress field within the liquid as it influences the intermolecular force field. The extended evaporating meniscus of a liquid thin film is generated out of these long rang intermolecular forces (Wayner et al. 1976; DasGupta et al. 1993; Sartre 2000). Derjaguin and Kussakov (1939) illustrated the use of augmented Young-Laplace equation to account for both the influences of liquid-vapor and liquid-solid interfaces on the effective pressure jump at the liquid-vapor interface. The augmented Young-Laplace equation relating pressure jump, capillary pressure and the intermolecular force field is presented below (DasGupta 1992; DasGupta et al. 1993; Schonberg and Wayner 1993; Wayner 1995; DasGupta et al. 1993).

$$P_l - P_v = \frac{B}{\delta^n} - \sigma K \qquad (1.1)$$

Where δ is the film thickness, K is the curvature and σ is the surface tension. $\frac{B}{\delta^n}$ is the disjoining pressure (also denoted as $-\Pi$) resulting due the presence of long range intermolecular forces between liquid and solid acting over small distances and are represented as follows (Deryagin and Churaev 1976; Argade et al. 2007).

For ultra-thin film region ($\delta \le 20\,\text{nm}$) of simple pure fluid, $\frac{B}{\delta^n} = \frac{A}{6\pi\delta^3} = -\Pi$ where A is the classical Hamaker constant and $B\left(= \frac{A}{6\pi} \right)$ is modified Hamaker constant. For thick film region, ($\delta \ge 40\,\text{nm}$), $\frac{B}{\delta^n} = \frac{B}{\delta^4} = -\Pi$ and B is the dispersion constant.

The extended meniscus of a liquid has three distinct regions, namely the adsorbed thin film ahead of the meniscus, the intrinsic meniscus region with a transition region in between. The different regimes of the evaporating film in the microgrooves are presented in Figure 1.5. In the non-evaporating zone, the disjoining pressure is strong and no evaporation takes place (DasGupta et al. 1993; Argade et al. 2007; Zhao et al. 2013). Capillary force plays an important role in the intrinsic meniscus (thicker end of the film), where the curvature of the film remains constant. The suction potential of an evaporating thin film is closely related to disjoining pressure. The main heat transfer occurs in the evaporating thin film region, where both capillary and disjoining forces are present, due to relatively small thermal resistance across the film (Wang et al. 2007).

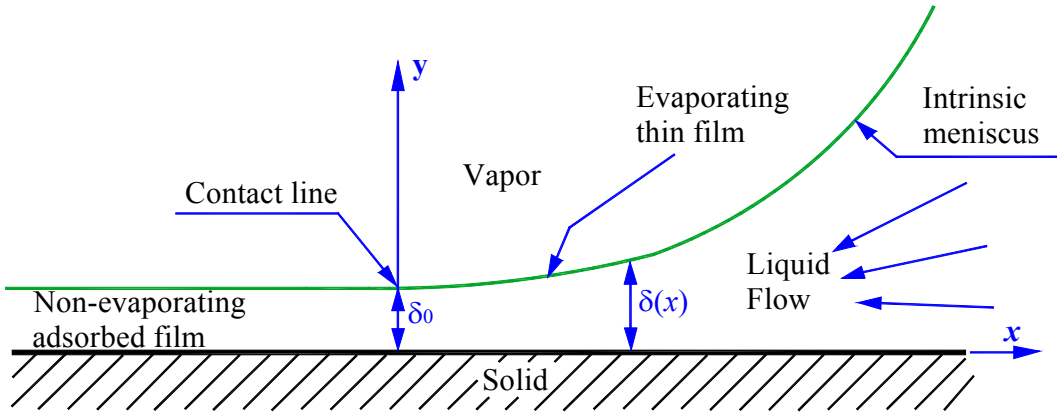

Figure 1.5. Schematic representation of the different regimes of the evaporating film in the microgrooves

1.3 OVERVIEW OF LITERATURE AND AIM OF THE PRESENT WORK

Micro heat pipe is a wickless, non-circular channel with micro-scale hydraulic diameter of the cross section so that the pressure gradient for flow along the length of the pipe is developed due to capillary and intermolecular force field changes. The geometry results in very high surface to volume ratio and highly efficient heat transfer (Faghri 1995; Khrustalev and Faghri 1994; Peterson 1994; Swanson and Peterson 1995; Dunn and Reay 1982; Moon et al. 2004; Tabeling 2004; Harirchian and Garimella 2009). Evaporation heat transfer characteristics in the micro region of a rotating miniature heat pipe have been widely studied by Faghri and his co-workers (Rahman and Faghri 1992; Faghri et al. 1993). The friction constant of the microchannels is greatly influenced by the cross-sectional aspect ratio. Experimental

friction factor in smooth trapezoidal microchannels, fabricated on silicon, was estimated by Wu and Cheng (2003) for laminar flow of deionized water. A correlation of laminar friction constant for trapezoidal microchannels in terms of the cross-sectional aspect ratio was also derived by them. Effects of functional surface on performance of a micro heat pipe were studied by Qu et al. (2008). Detailed theoretical analysis of capillary performance of triangular microgrooves has been executed by Sheu et al. (2004). Peterson and Ma (1996) analyzed the maximum heat transport in triangular microgrooves theoretically. They have also developed a mathematical model to find transport capability and temperature gradients that contribute to the overall axial temperature drop as a function of heat transfer in a micro heat pipe (Peterson and Ma 1999). An analytical model was proposed by Xu and Carey (1990) that can be used to predict heat transfer characteristics of evaporation of film on V-shaped microgrooves. Ha and Peterson (1996; 1998) developed an analytical expression for the evaporating film profile on microgrooves with non-uniform heat input. They used perturbation method to solve the axial flow of an evaporating thin film through a V-shaped microchannel with tilt. Wang et al. (2008) studied the total heat transfer in the thin-film region of an evaporating meniscus analytically. They also investigated the heat and mass transfer from an evaporating meniscus in a heated open groove (Wang et al. 2011).

Heat pipes with axial microgrooves is an attractive option that have been introduced for a wide variety of advanced thermal devices to transport heat through long distance, such as spacecraft thermal control systems (Chen et al. 2009). The main advantages of these devices are that these have powerful heat transfer capability and high effective thermal conductivity. Several experimental and theoretical studies have been performed using microgrooves of different cross sections to evaluate their performances (Babin et al 1990; Longtin 1994; Wang and Peng 1994; Badran et al. 1997; Moon 2002; Berre et al. 2003; Suman and Hoda 2005; Suman and Kumar 2005; Yang 2008; Panchamgam 2008; Chen et al. 2009; Hung and Tio 2012). Jiao et al. (2005; 2007) used trapezoidal-grooved heat pipes for their analysis. Some other researchers used triangular-grooved heat pipes (Kundu et al.2011; Stephan and Busse 1992; Ma et al. 1994; Ha and Peterson 1998; Ma and Peterson 1998; Suh et al. 2003). Do and Jang (2010) presented the effect of nanofluids on the thermal performance of a flat micro heat pipe with a rectangular grooved wick. They also developed a

mathematical model prior to analysis of the thermal characteristics of a flat micro heat pipe with a grooved wick (Do et al. 2008). Peng and Peterson (1996) worked with rectangular-grooved channels to investigate the liquid flow and heat transfer characteristics in microchannels. Deng et al. (2013) investigated the heat transfer characteristics of micro heat pipe array applied to flat plate solar collector experimentally. Ducan and Peterson (1995) experimentally optimized the fill ratio for triangular grooved micro heat pipe. Similar study has been theoretically performed by Suman (2006). Kang et al (2002a, 2002b, 2004) fabricated microchannels of different shapes and tested the performance of radial grooved micro heat pipe. Mallik et al. fabricated the vapor deposited micro heat arrays and investigated the same theoretically (Mallik and Peterson 1995; Mallik et al. 1995). Kundu et al. (2015) introduced an on-chip micro heat pipe that can be integrated directly to a semiconductor device without compromising its performance.

Change-of-phase heat transfer systems have the potential to provide cooling heat fluxes as high as several thousands of W/cm^2. It is important to mention in this context that the free energy of an ultra-thin film of liquid on a solid substrate is different from that of a bulk fluid because of the fact that the long-range intermolecular force field is a function of the thickness and curvature of the film (Derjaguin and Zorin 1957; Deryagin and Churaev 1976; Derjaguin et al. 1965; Pati et al. 2013). In addition, it may be noted that the fundamental physics that governs the operation of micro heat pipes arises from the difference in the capillary pressure across the liquid–vapor interfaces in the evaporator and condenser regions. Additionally, wettability and intermolecular interactions play crucial roles to define the performance of these microdevices utilizing evaporating curved microfilms on microgrooved surfaces (Chakraborty 2013). The foundation for studying of interfacial transport processes in thin film evaporation was laid by Derjaguin and his co-workers as well as the research group of Wayner (Wayner et al. 1976; Potash and Wayner 1972; Renk et al. 1978; Wayner 1980; Wayner 1991; Panchamgam et al. 2005). Derjaguin and Churaev (1978) evaluated the excess potential present in thin film of a liquid in terms of disjoining pressure, which is the effect of intermolecular forces of attraction and repulsion. A detailed review on evaporation coefficient of water was presented by Eames et al. (1997).

The heat transfer coefficient of an evaporating liquid film at the micro-region was evaluated by Wayner (1976). Holm and Goplen combined the model developed by Wayner with one dimensional analysis of the radial heat transfer through heat pipe walls considering trapezoidal grooves (Holm and Goplen 1979). Rossomme et al. (2008) developed a multi-scale numerical modeling of radial heat transfer in grooved heat pipe evaporators. Kundu et al. (2011) quantified the shape of the liquid meniscus in the microgrooves using image analyzing interferometry, as a function of heat input and opposing body forces. Hung and Tio (2012) have performed thermal analysis of a water-filled micro heat pipe with phase-change interfacial resistance. They have shown that heat transport capability of a micro heat pipe is dominated by phase-change heat transfer at the liquid–vapor interface (Kang et al. 1999). A detailed theoretical and experimental review of recent researches along with comparative analysis of the performance on micro heat pipes have been compiled by several researchers (Sobhan et al. 2007; Suman 2007).

With the ever expanding need to handle large heat fluxes; the integration of the micro heat pipe with the semiconductor components is important. Although large volume of literature exists indicated as above, all the above mentioned studies are dealt with microchannels mostly on non-silicon material (Schutze et al. 2001; Perret et al. 2002; Papautsky et al. 1998; Lim 2008; Stevanovic et al. 2010). Further, they cannot be integrated directly with the semiconductor devices to be functioning as micro heat pipe. The main challenge lies with the development of a micro heat pipes, generated out of optimized microchannels to be etched on the unused backside of the silicon of the semiconductor device, suitable for on-board integrability.

The primary objective of the present dissertation is the design and fabrication of on-chip micro heat pipes with the aid of microchannels etched on the unused backsides of the semiconductor devices, followed by its characterization and performance analysis. The studies in the present dissertation have been divided into three categories: A. Design and fabrication of various microchannels on silicon, leading to the development of the on-chip micro heat pipe B. Microscopic analysis of coolant spreading and thermal transport over microgrooved surface, and C. Performance analysis of on-chip micro heat pipe.

The thermal performance of the micro heat pipe can be significantly enhanced by integrating it with the electronic component itself, leading to a paradigm called *on-chip micro heat pipe*, for making it compact without compromising its performance. With the need of integration of micro heat pipes to the heat generating semiconductor devices itself, the optimized design and fabrication of micro heat pipe on silicon is important. This motivates the first objective of this dissertation which is to design and fabricate on-chip micro heat pipe using microchannels of varied shapes viz. rectangular, triangular and configurations such as straight, and radial on single crystalline silicon wafer.

Second, enormous amount of heat can be extracted exploiting change-of-phase heat-transfer processes, especially using thin film evaporation. This is because of the fact that the free energy of an ultra-thin liquid on a solid substrate is quite different from that of the bulk fluid. The long range intermolecular force in liquid thin film on a solid substrate is dominant and function of the thickness and curvature of the film (Derjaguin and Zorin 1957; Deryagin and Churaev 1976; Derjaguin et al. 1965; Kundu et al. 2011; Chatterjee et al. 2011). Further, the fundamental physics that governs the operation of micro heat pipes arises from the difference in the capillary pressure across the liquid–vapor interfaces in the evaporator and condenser regions. The performance of the microdevices that work utilizing the evaporating curved microfilms on microgrooved surface also depends on the intermolecular interactions and the wettability of the liquid on the solid substrate. This motivates the second objective of this dissertation, which is the quantification of the shape dependent intermolecular and surface force fields of an evaporating meniscus in the microgrooves using a non-obtrusive measurement technique, namely, image analyzing interferometry, as a function of heat input and opposing body forces.

Third, the rapid increase in the heat load signatures in electronic components in electronic packaging industry, micro gravity environments, and spacecraft thermal control systems demand effective and compact cooling strategies. The performance testing of the developed micro heat pipe before on-board integration is important. This motivates the third objective of this dissertation which is to evaluate the cooling potential of the micro heat pipe.

1.4 PROBLEM DEFINITIONS AND OUTLINE OF THE THESIS

With the aforementioned motivations in mind, a heat transfer cell is specifically designed to analyze the heat spreading capacity of a microgrooved surface. V-shaped microgrooves are etched on silicon wafers using standard lithographic process. The shapes of the liquid menisci in the microgrooves are accurately measured using image analyzing interferometry as functions of heat input and opposing body force (angle of inclination). The relevant parameters that govern the spreading and cooling process of an evaporating curved microfilm e.g., the adsorbed film thickness, contact angle and curvature at the thicker end of the meniscus are accurately measured. The trends in these values are found to be consistent with the physics of the process. The temperature profiles are measured for the microgrooved and non-grooved silicon substrates under identical conditions of heat input and inclination and the enhanced spreading of the film in presence of microgrooves towards the hot region is quantified. The axially average values of a dimensionless temperature, defined for this study, are used to quantify the enhanced cooling and temperature homogenization potentials of microgrooved surfaces along with the effect of opposing body forces.

In the next step, the performance of a specially fabricated micro heat pipe is analyzed to evaluate its enhanced cooling potential. Triangular microgrooves are etched on a silicon wafer via a lithographic process with two reservoirs at the two ends of the microchannel array. The top of the microgroove is closed by a thin Pyrex glass (Pyrex 7740) using anodic bonding. Electrochemical spark erosion technique is used to create holes on the Pyrex for vacuum connections and for coolant insertion. The cooling potential of the micro heat pipe is evaluated by accurately measuring the temperature distributions along the channel length at different values of the applied heat load. The capillary suction capability of the micro heat pipe is further probed with the help of a proposed mathematical model by evaluating the axial variation of the radius of curvature of the evaporating liquid film. The remaining part of the thesis is organized in the following manner.

- In Chapter 2, the complex fabrication processes are discussed in detail and subsequently, the design and development of the on-chip micro heat pipe with their important steps are presented.

- In Chapter 3, the design and development of experimental cells along with the attachments of appropriate measurement devices are presented.
- In Chapter 4, the microscopic and macroscopic studies on spreading and cooling over the fabricated microgrooved surface are presented. The performance of the on-chip micro heat pipe is studied both theoretically and experimentally.
- Finally, in Chapter 5, important inferences drawn from the studies executed in the present thesis and the scopes of further works are presented.